



PARIS 2017

## We A3 04

### Imaging Beneath a Gas Cloud in the North Sea without Conventional Tomography

C. Ravaut\* (Statoil ASA), F.A. Maaø (Statoil ASA), J. Mispel (Statoil ASA), A. Osen (Statoil ASA), M. Warner (Imperial College London), L. Guasch (S-Cube, London), T. Nangoo (S-Cube, London)

## Summary

---

To reduce sensitivity of full-waveform inversion to cycle skipping, new objective functions have been introduced in the last couple of years. We here investigate the capability of adaptive waveform inversion (AWI) based on Wiener coefficients which we apply to a gas cloud field in the North Sea. The objective of this work is to evaluate if AWI can start from a simple 1D like initial velocity model and produce reasonable migrated images. To do so we compare the results from FWI starting from a well-defined reflection tomography model with the results derived from AWI starting from a simple 1D initial model. The quality of the results is evaluated using RMO cubes derived from 3D Kirchhoff PSDM common image gathers. We here demonstrate that, in this gas-cloud context, AWI is able to reconstruct a well resolved velocity in the gas cloud starting from the 1D like model. The quality of the P-wave velocity model is better than the velocity model derived from tomography and similar to the one derived by tomography plus FWI. For this case, we show that AWI could replace tomography for model building thus reducing the project duration.



## Introduction

Defining an initial velocity model to ensure success of full-waveform inversion (FWI) can be a difficult task due to the sensitivity of the method to cycle skipping. In most imaging projects, initial velocity models for FWI are derived from reflection tomography. Nevertheless, in complex geological contexts, for example gas clouds, event picking for tomography can be a challenging task and tomography may contain short wavelength velocity errors. In addition, several pre-processing steps are needed to run reflection tomography that add to the project duration.

To avoid cycle skipping in FWI, new objective functions based on cross-correlation (Van Leeuwen and Mulder, 2010), Wiener filters, or the optimal transport method (Métivier et al., 2016) have been recently introduced. All these methods seem to reduce the sensitivity of waveform inversion to cycle skipping at least on synthetic examples. In this paper, we focus on the objective function based on Wiener coefficients (adaptive waveform inversion – AWI) proposed by Warner and Guasch (2014) which we apply to a gas-cloud field in the North Sea. Warner and Guasch (2014) used AWI to start from a reflection tomographic initial model; here, we investigate if AWI can start from a simple 1D model. We compare the results from FWI using the reflection tomography initial model with those obtained from AWI when starting from a very simple 1D-like model. The quality of the results is evaluated using Kirchhoff-migrated images and associated Residual Move Out (RMO) maps. In the context of gas clouds, our objective is to investigate if tomography can be avoided entirely to derive the initial P-wave velocity model and if the model from AWI alone is as good quality as the one defined using a more classical approach including tomography.

## Methodology and application to a North Sea dataset

Both AWI and FWI inversion methods are implemented in the same 3D VTI acoustic waveform inversion code; only the objective functions are different. For FWI, the objective function is a classical least-square misfit. For AWI, Wiener filters are used to match predicted and observed data. The misfit is defined so that it forces the filter coefficients to become zero-lag delta functions (Warner and Guasch, 2016). For FWI, we precondition the gradient by using the diagonal term of the Hessian, whereas for AWI, no illumination compensation is applied to the gradient.

We applied FWI and AWI to a 3D OBN dataset acquired in the North Sea. Previous studies over this field have demonstrated the potential of these methods to better reconstruct the gas cloud when using an initial reflection tomography model (Ratcliff et al., 2011; Warner et al., 2013). Here we investigate the capability of AWI to start from a 1D-like initial model. To do so, we run both FWI and AWI in parallel and compare the derived P-wave velocity models. To estimate the quality of our results, we compare RMO cubes obtained from 3D Kirchhoff PSDM common image gathers for initial and final models. For our inversions, the source wavelet is estimated outside the FWI or AWI iterations, following Skopintseva et al. (2016). As the water layer is extremely shallow, the source bubble is included in the arrivals used for the source estimation. The wavelet is estimated from low-frequency data and the full trace length is used.

For FWI, we used the reflection tomography initial model defined in Warner et al. (2013). In this model, the gas cloud is already well defined. For AWI, the 1D-like initial model is built by heavy smoothing of the tomography model to remove the gas cloud (figure 3a). In both tests, the 1D anisotropy models are defined in the same way using a well-log located outside the gas cloud. Both epsilon and delta models are quite simple and could be better defined to improve the quality of the final migrated images. Both inversions are run with the same input parameters. Only P-wave velocities are inverted, using a frequency range from 3.0 to 6.5 Hz. Offsets from 1.2 to 10.5 km are included and late arrivals at very near offsets are muted away. For larger offsets, reflections are included in the data. Data selection for one shot gather is illustrated in figure 1. It is interesting to note that the input data have very little pre-processing applied. Only a simple frequency filter is applied to remove low frequency noise and high frequency data. No de-multiple or PZ sum are applied to the data before the inversion. For both tests, the same Gaussian smoother is applied to the

gradient at each iteration; 50 iterations are run for AWI and 30 iterations for FWI. The initial and the final P-wave velocity models from each test are used to migrate the data using a 3D VTI Kirchhoff pre-stack depth migration. The migrated common image gathers (CIG) are used to compute RMO cubes for each model (figures 2c, 2f, 3c & 3f). In these cubes, red picks represent over-migrated gathers indicating too-fast velocities, blue picks represent under-migrated gathers indicating too-low velocities and yellow picks represent flat gathers.

## Results and discussion

As expected the initial 1D-like velocity model creates strong cycle skipping between the observed and the synthetic dataset as illustrated in figure 1a. The phase difference is quite large for the reflected and refracted energy at near and large offsets. Intermediate offsets are better fitted by the initial model.

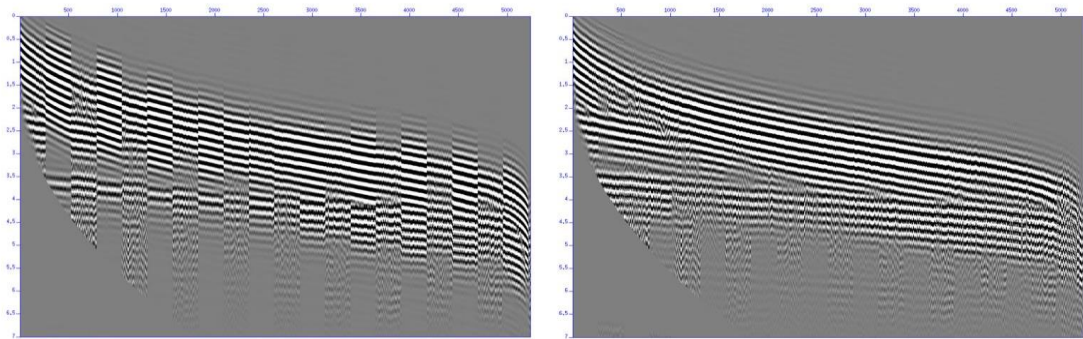


**Figure 1** Shot gather showing interleaved observed and synthetic data for a) 1D-like initial velocity model, b) P-wave velocity model reconstructed after 50 iterations of AWI. Data are interleaved every 20 traces starting from the real data.

When starting FWI from this initial velocity model, the inversion ends up in a local minimum and only the very shallow part of the model is updated. Starting with a lower frequency range from 3.0 to 4.5 Hz does not solve the issue. Using the tomography initial model (figure 2a) to run FWI converges towards a better velocity model (figure 2d). In this case, the phase difference between observed and synthetic data is much less, especially for the reflected energy, and the inversion is able to reconstruct a more detailed gas cloud. Another possibility would be to apply a different time windowing to the data in order to limit the cycle skipping related to the reflected energy when starting from the 1D model. We did not try this option as our objective here is to reduce the workflow steps and pre-processing applied to the data before the inversion. The migrated image from FWI (figure 2e) is better defined in the gas and below than the migrated image using the tomography model (figure 2b). The RMO maps show more yellow picks in the gas cloud area (figure 2f). Nevertheless, to the right of the gas cloud, red picks between 2.2 and 2.8 km depth seem to correlate with some artefacts in the FWI model (red dashed circle in figure 2b) probably due to the acquisition geometry. In this study, we did not make any efforts to remove these artefacts from the FWI model before migration. These acquisition artefacts could be attenuated by increased smoothing or by introducing more regularization to the gradient.

In all RMO maps, red picks on the right side of the gas cloud can also be observed between 600 and 1300 m depth in figure 2 and 3. As both FWI and AWI do not improve the image in this region, it is reasonable to suppose that these picks may be related to the inaccuracy of our anisotropic parameters as we are using a 1D vertical profile to define epsilon and delta. This is due to our objective to work from 1D initial models. One way to improve imaging in these regions could be to invert for epsilon with AWI or FWI after P-wave inversion.

When using AWI from the 1D-like initial model (figure 3a), the inversion is able to reconstruct the gas cloud (figure 3c). Looking at observed and synthetic data after inversion we see that AWI has explained most of the data and has completely recovered from cycle skipping (figure 1b). Both

refracted and reflected energy are well explained. Comparing the migration and RMO results, we can see that AWI is reconstructing a good velocity model. The RMO picks for AWI are flatter in the gas cloud than in the initial 1D model. The migrated image from the AWI inversion shows better definition of the gas cloud and the areas above and below (figure 3e). The horizon sag below the top of the gas (figure 3b, blue arrow) is flat on the migrated image after AWI inversion (figure 3e). Compared to the tomography model, the AWI velocity model in the gas cloud itself has a more geological character showing more continuous reflectors (figure 3e). RMO picks are flatter in the gas cloud in figure 3f than in figure 2c. On the side of the gas, RMO picks are less flat for AWI than tomography but with limited impact on the image quality.

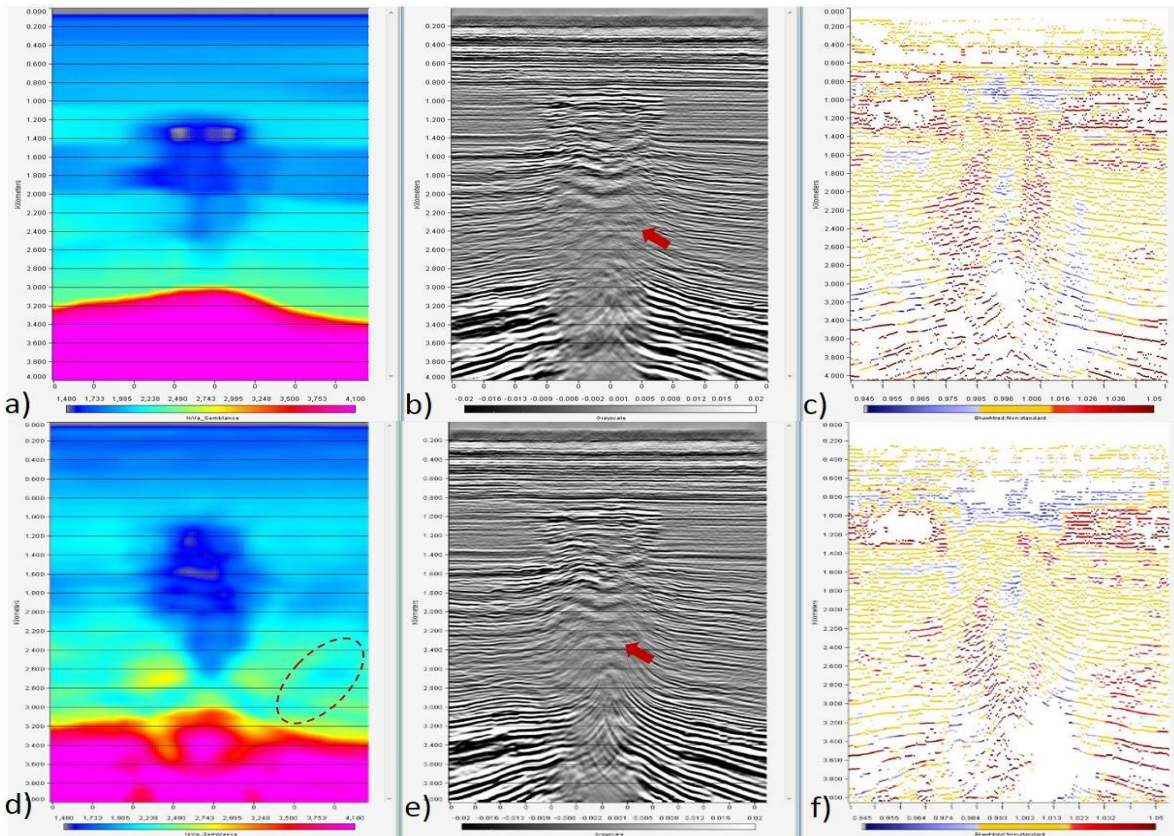


**Figure 2** Results from tomography (a, b, c) and tomography followed by 30 iterations of conventional FWI (d, e, f). Left: final velocity models. Centre: corresponding migrations. Right: RMO maps. Red is over-migrated, Blue is under-migrated, Yellow is correctly migrated, White has no picks.

Compared to FWI, AWI recovers a good gas velocity down to about 2.8km depth (same quality of RMO picks in the gas in figure 2f and 3f). The horizons around 2.4 km depth show more continuity and seem to form an anticline on migration after both FWI and AWI (red arrows figure 2e and figure 3e). On the left side of the gas cloud, AWI results are probably contaminated by small artefacts due to acquisition geometry. On the FWI model, artefacts associated with the finite aperture of the acquisition are visible on the model (red circles figure 2d) and on the migration. On the AWI model this imprint of the acquisition is less pronounced. The artefacts on the AWI results are of smaller wavelength than the ones observed on the FWI results. The lateral extent of the gas and its vertical resolution are also different on both models as AWI is starting further from the true model than FWI. Here, we are comparing 50 iterations from AWI with 30 iterations from FWI. More iterations of AWI might be necessary to get a velocity model as well resolved as the model derived from FWI.

## Conclusions

In this study we have demonstrated that, in a gas-cloud context, AWI is able to reconstruct a well resolved velocity model starting from a very simple 1D-like initial model. In this case, very little pre-

processing is applied to the data and there is minimal effort applied to time-window the data. The quality of the derived P-wave velocity model is better than the tomographic one and is similar to that derived by tomography plus FWI. For this case, AWI could replace tomography for model building. Depth imaging could start earlier without requiring much effort in data processing for model building.

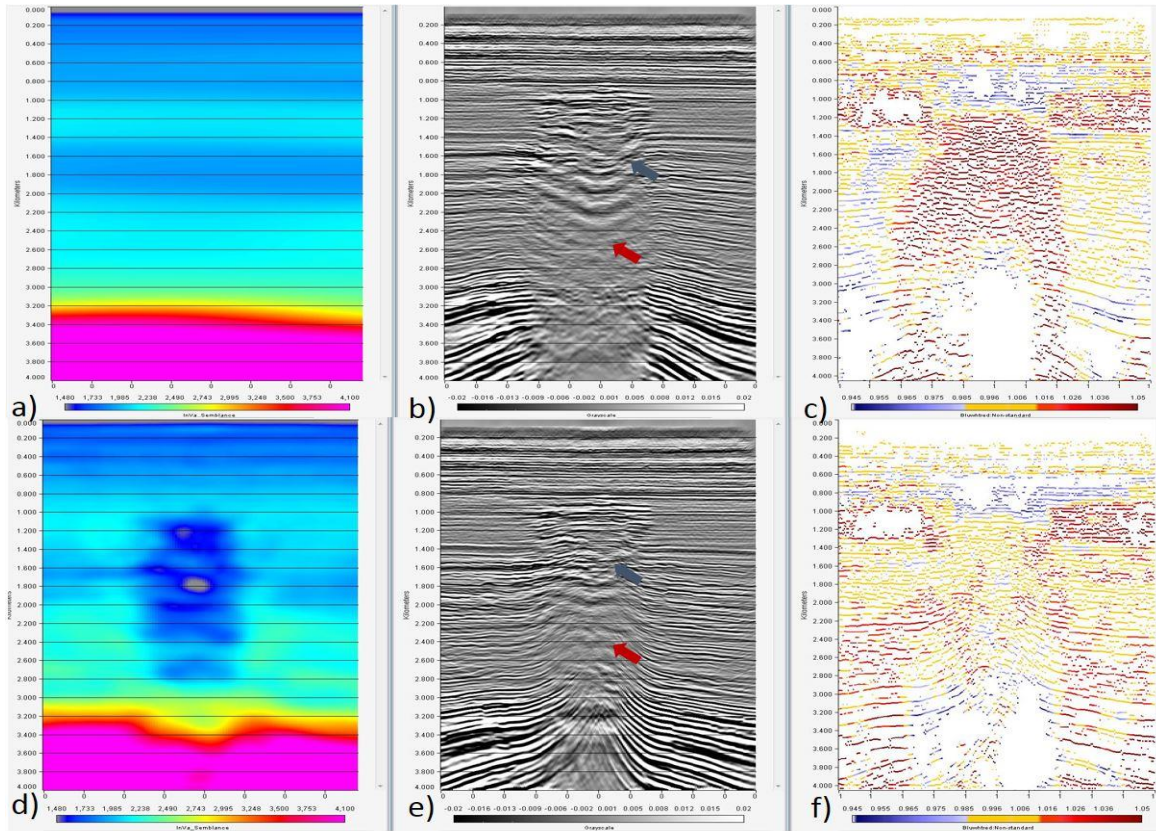


**Figure 3** Results from a simple 1D-like model (a, b, c) and AWI starting from this model (d, e, f). Left: velocity models. Centre: corresponding migrations. Right: RMO maps.

## Acknowledgments

Thanks to Krishna Ramani (WG) for help with migration. We also thank the Statoil FWI team for the implementation of FWI. We acknowledge Statoil and S-Cube for permission to present this paper. The AWI methodology described here is the subject of GB patent number GB1319095.4

## References

- Métivier L., Brossier R., Mérigot Q., Oudet E. and Virieux J (2016) Measuring the misfit between seismograms using an optimal transport distance: application to full waveform inversion. *Geophysical Journal International* 205.1: 345-377.
- Ratcliffe, A., Win, C., Vinje, V., Conroy, G., Warner, M., Umpleby, A., & Bertrand, A. (2011). Full waveform inversion: A North Sea OBC case study. *SEG Annual Meeting*.
- Skopintseva, L. V., F. A. Maaø, and Ø. Pedersen (2016). Importance of the Source Estimation in FWI: Sensitivity and Examples. *78th EAGE Conference and Exhibition*.
- Van Leeuwen, Tristan, and W. A. Mulder (2010). A correlation-based misfit criterion for wave-equation traveltime tomography. *Geophysical Journal International* 182.3: 1383-1394.
- Warner, M., Ratcliffe, A., Nangoo, T., Morgan, J., Umpleby, A., Shah, N., ... & Conroy, G. (2013). Anisotropic 3D full-waveform inversion. *Geophysics*, 78(2), R59-R80.
- Warner M., and Guasch L. (2014) Adaptive waveform inversion. 84<sup>th</sup> SEG Annual meeting
- Warner M., and Guasch L. (2016) Adaptive waveform inversion: Theory. *Geophysics*, 81, R429-R445